HEAT TRANSFER ANALYSIS IN MHD THERMAL NANOFLUID USING KELLER-BOX METHOD

Muhammad Imran Anwar[2,3], Nida Tanveer[2], I. Khan[1] and Waqar A Khan[4]

[1]Faculty of Mathematics and Statistics, Ton Duc Thang University, Ho Chi Minh City, Vietnam.
[2]Department of Mathematics, Faculty of Science, University of Sargodha, Pakistan,

[3]Higer Education Department (HED) Punjab , Pakistan,

[4]Department of Mechanical Engineering, College of Engineering, Prince Mohammad Bin Fahd University I P.O. Box 1664, Al Khobar 31952, Kingdom of Saudi Arabia

*Corresponding author: email: ilyaskhan@tdt.edu.vn

Abstract

Thermal radiation analysis in MHD Casson nanofluid flow over an exponentially stretching sheet is investigated. A chemical reaction is also considered. A non-uniform magnetic field of strength is imposed in a transverse direction. The governing boundary layer equations are reduced into ordinary differential equations by using suitable similarity transformations. The coupled nonlinear equations are solved numerically using an implicit finite difference scheme by means of the Keller-box method. A comparison of the obtained results is performed with the published results. It is found that velocity profiles are suppressed with the increasing values of Hartmann number and Casson fluid parameter.

***Keywords**: Thermal nanofluid; Radiation; MHD; Chemical reaction; Stretching sheet; Keller-box method*

1. Introduction:

In nanofluid studies the idea of Buongiorno [1] has received special attention specially from theoretical researchers. He studied nnaofluid to increase its thermal conductivity in comparison with the base fluid and found that the Brownian motion and thermophoresis effects in the base fluid enhances the thermal conductivity of the liquid. Khan and Pop [2] firstly investigated the flow of the nanofluid together with Brownian and thermophoresis motion on the stretching surface. Yu et al. [3] summarized and lightened progress on the study of nanofluids and opportunities for future research such as the preparation methods, the evaluation methods for the stability of nanofluids and the ways to enhance the stability for nanofluids, the stability mechanisms of nanofluids etc. Makinde et al. [4] studied numerically the effect of suction, viscous dissipation, thermal radiation and thermal diffusion on the boundary layer flow of the nanofluid over a moving plate. Babu et al. [5] discussed the various effects of parameters like particle size, volume fraction, material etc. and different mechanisms to enhance the heat transfer qualities for Brownian motion, thermophoresis and clustering of nanoparticles.

The flow over a stretching surface has important applications in many engineering processes such as extrusion, melt-spinning, the hot rolling, wire drawing, glass fiber production, manufacture of plastic and rubber sheets, cooling of a large metallic plate in a bath, which may be an electrolyte etc. Sakiadis [6] introduced his pioneering work with a study of boundary layer behavior on continuous solid surfaces. Further Fox et al. [7] extended the work of Sakiadis to investigate the laminar boundary layer flow on a moving continuous surface with suction and injection. Gupta et al. [8] enhanced the study and investigated heat and mass transfer on a stretching sheet with suction and blowing. Rajagopal et al. [9] studied the flow of an incompressible second-order fluid past a stretching sheet. Dutta et al. [10] made an anylsis of temperature distribution in the flow of a viscous incompressible fluid. Magyari et al. [11] described boundary layers on an exponentially stretching continuous surface with an exponential temperature distribution. Bidin et al. [12] investigated numerically the effect of thermal radiation on the steady laminar two-dimensional boundary layer flow and heat transfer over an exponentially stretching sheet. Ishak [13] studied MHD boundary layer flow due to an exponentially stretching sheet with radiation effect.

The Keller Box scheme for the solution of parabolic boundary layer equations is both accurate and robust. It has been extensively used in solving broad class of problems including convection flows, jet flows, turbulent boundary layer as well as seprating flows. Keller Box scheme has advantages in mathematics and physics:

- This scheme is implicit with 2nd order accuracy.
- It is efficient for the parabolic partial differential equation.
- The accuracy of this method has been studied for incompressible and compressible, laminar and turbulent boundary layer past two dimensional and axisymmetric bodies.
- Keller Box can be advantageous for security issues in networking.

Motivated by the above investigations, the present work concerned with the the chemical reaction and radiation effects on MHD Casson nanofluid flow over an exponentially stretching sheet. By applying the suitable similarity transformations, the system of nonlinear partial differential equations are reduced into the system of nonlinear ordinary differential equations. Nondimensional physical parameters namely Casson fluid parameter , Hartmann number, radiation parameter, chemical reaction parameter, Prandtl number, Thermophoresis parameter, Brownian motion parameter and Lewis number appear after reduction along with the system of coupled nonlinear ordinary differential equations. Coupled equations are then solved numerically by using Keller Box method. A comparison of the present work with the previously published result and the behavior of each physical parameter are shown through tables and graphs.

2. Problem Formulation

Consider a steady, viscous, incompressible, two-dimensional boundary layer flow of Casson nanofluid over an exponentially stretching sheet. The stretching and free stream velocities are assumed to be of the forms $u_w(x) = a\exp(x/l)$ and $u_\infty(x) = 0$ respectively. , where a is constant, x is the coordinate measured along the stretching surface and l is the length of the sheet. The temperature T and the nanoparticles fraction C take constant values T_w and C_w, respectively at the wall, whereas the ambient values of temperature T_∞ and the nanoparticles fraction C_∞ are attained as y tends to infinity. A non-uniform magnetic field of strength $B(x) = B_0\exp(x/2l)$ is imposed in transverse direction (normal to the flow direction), where B_0 is the uniform magnetic field strength. It is assumed here that the induced magnetic field due to the motion of an electrically conducting fluid is negligible. Further, external electrical field is zero and the electric field due to the polarization of charges is negligible.

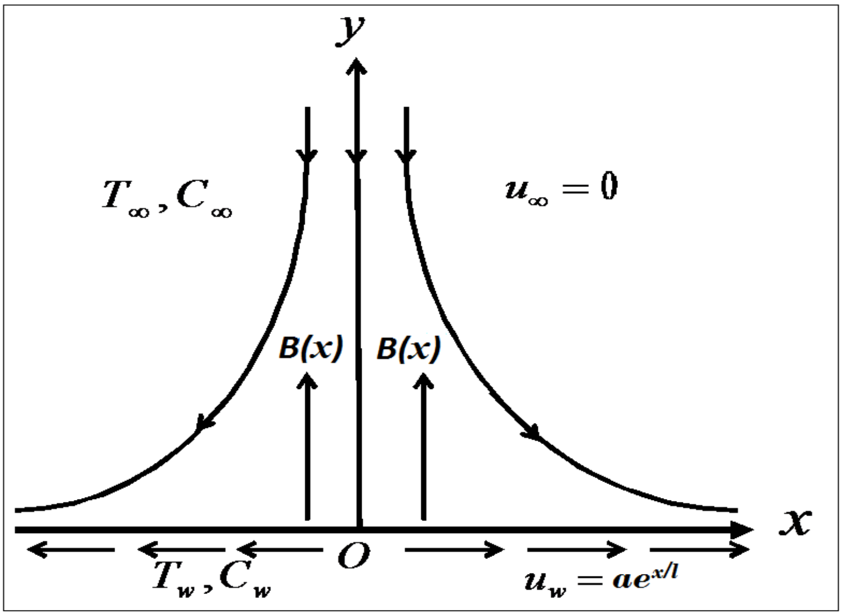

Figure 1: Physical Model

The governing boundary layer equations are as follows

$$\frac{\partial u}{\partial x} + \frac{\partial v}{\partial y} = 0, \tag{1}$$

$$u\frac{\partial u}{\partial x} + v\frac{\partial u}{\partial y} = \nu\left(1+\frac{1}{\beta}\right)\frac{\partial^2 u}{\partial y^2} - \frac{\sigma\, B^2(x)}{\rho_f}u, \tag{2}$$

$$u\frac{\partial T}{\partial x} + v\frac{\partial T}{\partial y} = \alpha\frac{\partial^2 T}{\partial y^2} - \frac{1}{(\rho c)_f}\frac{\partial\, q_r}{\partial y} + \tau\left[D_B\frac{\partial C}{\partial y}\frac{\partial T}{\partial y} + \frac{D_T}{T_\infty}\left(\frac{\partial T}{\partial y}\right)^2\right] + \frac{\mu}{\rho c_p}\left(1+\frac{1}{\beta}\right)\left(\frac{\partial u}{\partial y}\right)^2, \tag{3}$$

$$u\frac{\partial C}{\partial x} + v\frac{\partial C}{\partial y} = D_B\frac{\partial^2 C}{\partial y^2} + \frac{D_T}{T_\infty}\frac{\partial^2 T}{\partial y^2} - K_1(C - C_\infty). \tag{4}$$

where u and v are the velocity components along the x - and y - directions respectively, υ is the kinematic viscosity, σ is the electrical conductivity, B_0 is the strength of the magnetic field, C is the species concentration in the base fluid, ρ_f is the fluid density of the base fluid, $\alpha = k/(\rho c)_f$ is the thermal diffusivity, D_B is the Brownian diffusion coefficient, D_T is the thermophoretic diffusion coefficient, K_1 is the chemical reaction parameter and $\tau = (\rho c)_p/(\rho c)_f$ is the ratio of effective heat capacity of the nanoparticle material to the effective heat capacity of the base fluid and

$\beta = \mu_\beta \sqrt{2\Pi c} \Big/ p_y$ is Casson fluid parameter(Non-Newtonian parameter). Π_c is the critical value of the product of the strain tensor with itself. In case of Casson fluid flow $\Pi > \Pi_c$ [14,15] as the particular amount of stress is to be applied to move Casson fluid such as tooth paste, honey, jelly etc. . Where P_y is known as yield stress of the fluid and mathematically can be expressed $P_y = \mu_B \sqrt{2\Pi} \Big/ \beta$. Here μ_B is plastic dynamic viscosity of the fluid. Casson fluid exhibit the yield stress as it is the property of elastic fluids. If the shear stress is less than the yield stress applied to it then Casson fluid behaves like a solid whereas if the shear stress is greater than the yield stress then it starts to move.

Here ϕ_v is the viscous dissipation function defined as

$$“\phi_v = 2\left[\left(\frac{\partial u}{\partial x}\right)^2 + \left(\frac{\partial v}{\partial y}\right)^2 + \left(\frac{\partial w}{\partial z}\right)^2\right] + \left(\frac{\partial u}{\partial y} + \frac{\partial v}{\partial x}\right)^2 + \left(\frac{\partial v}{\partial z} + \frac{\partial w}{\partial y}\right)^2 + \left(\frac{\partial w}{\partial x} + \frac{\partial u}{\partial z}\right)^2 - \frac{2}{3}(\nabla \cdot u)^2”.$$

where the Rosseland approximation(radiation flux) is defined as:

$$q_r = -\frac{4\sigma^*}{3k^*}\frac{\partial T^4}{\partial y}, \tag{5}$$

where σ^* is the Stefan-Boltzmann constant and k^* is the mean absorption coefficient. It is assumed that temperature difference between the free steam T_∞ and local temperature T is small enough, expanding T^4 in Taylor series about T_∞ and neglecting higher order terms results

$$T^4 \cong 4T_\infty^3 T - 3T_\infty^4. \tag{6}$$

After substituting Eqs. (9) and (10), Eq. (7) reduces to;

$$u\frac{\partial T}{\partial x} + v\frac{\partial T}{\partial y} = \left(\alpha + \frac{16\sigma^*}{3k^*(\rho c)_f}\right)\frac{\partial^2 T}{\partial y^2} + \frac{\mu}{\rho c_p}\left(1 + \frac{1}{\beta}\right)\left(\frac{\partial u}{\partial y}\right)^2 \tag{7}$$

The subjected boundary conditions to this problem are

$$u = u_w(x) = ae^{\frac{x}{\ell}}, v = 0, T = T_w(x), C = C_w(x) \qquad at \qquad y = 0,$$

$$u \to 0, v \to 0, T \to T_\infty, C \to C_\infty \qquad as \qquad y \to \infty. \tag{8}$$

The prescribed temperature and concentration on the surface of stretching sheet are assumed to be of the form $T_w(x) = T_\infty + T_0 \exp(x/2l)$ and $C_w(x) = C_\infty + C_0 \exp(x/2l)$ where T_0 and C_0 are the reference temperature and concentration resp.

The nonlinear partial differential equation are reduced into nonlinear ordinary differential equations. For the sake of this purpose the stream function $\psi = \psi(x, y)$ is defined as

$$u = \frac{\partial \psi}{\partial y}, \quad v = -\frac{\partial \psi}{\partial x}, \tag{9}$$

where the continuity Eq.(1) is satisfied identically. Using the similarity transformations

$$\psi = \sqrt{2\ell \upsilon a} e^{\frac{x}{2\ell}} f(\eta) \qquad , \qquad \theta(\eta) = \frac{T - T_\infty}{T_w - T_\infty},$$

$$\varphi(\eta) = \frac{C - C_\infty}{C_w - C_\infty} \qquad , \qquad \eta = y\sqrt{\frac{a}{2\upsilon\ell}} e^{\frac{x}{2\ell}}. \tag{10}$$

On substituting Eqs. (9) and (10) in to Eqs. (2), (4) and (7) reduces to the nonlinear ordinary differential eqs.

$$\left(1 + \frac{1}{\beta}\right) f''' + ff'' - 2f'^2 - Mf' = 0, \tag{11}$$

$$Pr_N \theta'' + f\theta' - f'\theta + Ec\left(1 + \frac{1}{\beta}\right) f''^2 + Nb\theta'\phi' + Nt\theta'^2 = 0 \tag{12}$$

$$\phi'' + Lef\phi' - Lef'\phi + Nt_b\theta'' - LeR\phi = 0. \tag{13}$$

Where

$$\nu = \frac{\mu}{\rho_f}, Pr = \frac{\nu}{\alpha}, Le = \frac{\nu}{D_B}, Ec = \frac{u_w^2}{C_p(T_w - T_\infty)}, Nt_b = \frac{Nt}{Nb},$$

$$Nb = \frac{\tau D_B(C_w - C_\infty)}{\nu}, Nt = \frac{\tau D_T(T_w - T_\infty)}{\nu T_\infty}, R = \frac{2lK_1}{u},$$

$$M = \frac{2l\sigma B_0^2}{a\rho_f}, Pr_N = \frac{1}{Pr}\left(1 + \frac{4}{3}N\right), N = \frac{4\sigma^* T_\infty^3}{kk^*}. \tag{14}$$

Here, prime denote the differentiation with respect to η, ν is the kinematic viscosity of the fluid, Pr is the Prandtl number, *Le* is the Lewis number, *Ec* is the Eckert number, *Nb* is the Brownian motion parameter, *Nt* is the thermophoresis parameter, *M* is Hartmann number, *N* is the radiation parameter *R* is chemical reaction parameter and the corresponding boundary conditions (8) are transformed into;

$$f(\eta) = 0, f'(\eta) = 1, \theta(\eta) = 1, \phi(\eta) = 1 \qquad at \qquad \eta = 0,$$

$$f'(\eta) \to 0, \theta(\eta) \to 0, \phi(\eta) \to 0 \qquad as \qquad \eta \to \infty. \tag{15}$$

The important quantities of physical interest are the Skin-friction coefficient C_f, Nusselt number *Nu* and Sherwood number *Sh* defined as

$$C_f = \frac{\tau_w}{\rho U_w^2},\ Nu = \frac{xq_w}{k(T_w - T_\infty)},\ Sh = \frac{xq_m}{D_B(C_w - C_\infty)}. \tag{16}$$

Where τ_w is the wall shear stress, q_w is the wall heat flux and q_m is the wall mass flux are given by

$$\tau_w = \mu_B\left(1+\frac{1}{\beta}\right)\left(\frac{\partial u}{\partial y}\right)_{y=0},\ q_w = -k\left(\frac{\partial T}{\partial y}\right)_{y=0},\ q_m = -D_B\left(\frac{\partial C}{\partial y}\right)_{y=0} \tag{17}$$

Using the transformed variables (10), the non-dimensional expressions for the Skin friction coefficient $C_{fx}(0) = \left(1+\frac{1}{\beta}\right)f''(0)$, reduced Nusselt number $-\theta'(0)$ and reduced Sherwood number $-\phi'(0)$ respectively defined as

$$C_{fx}(0) = \sqrt{\frac{2l}{x}Re_x}C_f,\ -\theta'(0) = \frac{Nu}{\sqrt{(\frac{x}{2l})Re_x}},\ -\phi'(0) = \frac{Sh}{\sqrt{(\frac{x}{2l})Re_x}}. \tag{18}$$

Where $Re_x = U_w x/\upsilon$ is the local Reynolds number based on the stretching velocity. The transformed nonlinear ordinary differential Eqs. (11) to (13) subjected to the boundary conditions (15) are solved numerically by using the Keller-box method.

3. Results and Discussions

The coupled nonlinear ordinary differential Eqs. (11) to (13) subjected to the boundary conditions (15) are solved numerically by using the finite difference scheme name as the Keller Box method. The numerical results for pertent flow parameters for Brownian motion parameter Nb, thermophoresis parameter Nt, Casson fluid parameter β, Eckert number Ec, Chemical reaction parameter R, radiation parameter N, Prandtl number Pr, Lewis number Le and Hartmann number M are given in tabular form. Table 1 describes a comparison of the reduced Nusselt number $-\theta'(0)$ with the results given by Bidin and Nazar [12] and Ishak [13]. Table 2 shows the variations of the reduced Nusselt number $-\theta'(0)$, the reduced Sherwood number $-\phi'(0)$ and Skin-friction coefficient $C_{fx}(0)$ for different values of Nb, Nt, Pr, Le, β, *Ec*, M, *N* and *R*. It is noted that the reduced Nusselt number $-\theta'(0)$ decreases for increase in *Nb*, *Ec*, M, *R* whereas increases for increase in *Nt*, β, Pr, *Le* and *N*. Where the reduced Sherwood number $-\phi'(0)$ decreases for increase in *Nt*, β, *M*, *N* whereas increases for increase in *Nb*, *Ec*, *Le*, Pr, and *R*. Further the skin-friction coefficient $C_{fx}(0)$ decreases for increase in Pr, *M*, *N* and increases for increase in β and *Le*.

Table 1: Comparison of the reduced Nusselt number $-\theta'(0)$ when *Nb*= *Nt*= *Le* =*R* =*Ec*= 0 and $\beta \to \infty$.

Pr	M	N	Bidin and Nazar[12]	Ishak[13]	Present Results
			$-\theta'(0)$	$-\theta'(0)$	$-\theta'(0)$
	0	0	0.9548	0.9548	0.9548
	0	0	1.4714	1.4714	1.4714
	0	0	1.8691	1.8691	1.8691
	0	1.0	0.5315	0.5312	0.5312
	1.0	0	-	0.8611	0.8611
	1.0	1.0	-	0.4505	0.4505

Table 2: Variations of the local Nusselt number $-\theta'(0)$, the local Sherwood number $-\phi'(0)$ and Skin-friction coefficient $C_{fx}(0)$.

Nb	Nt	β	Pr	Ec	Le	M	N	R	$-\theta'(0)$	$-\phi'(0)$	$C_{fx}(0)$
0.1	0.1	5.0	6.5	0.5	5.0	0.1	0.1	0.1	1.0944	2.3719	1.2059
0.5	0.1	5.0	6.5	0.5	5.0	0.1	0.1	0.1	0.3212	2.6761	1.2059
0.1	**0.5**	5.0	6.5	0.5	5.0	0.1	0.1	0.1	0.6421	2.6694	1.2059
0.1	0.1	**7.0**	6.5	0.5	5.0	0.1	0.1	0.1	1.0994	2.3595	1.2357
0.1	0.1	5.0	**10.0**	0.5	5.0	0.1	0.1	0.1	1.0996	2.4181	1.2059
0.1	0.1	5.0	6.5	**0.9**	5.0	0.1	0.1	0.1	0.3507	2.9240	1.2059
0.1	0.1	5.0	6.5	0.5	**10.0**	0.1	0.1	0.1	1.0025	3.7595	3.7595
0.1	0.1	5.0	6.5	0.5	5.0	**2.5**	0.1	0.1	0.0117	2.9903	1.8617
0.1	0.1	5.0	6.5	0.5	5.0	0.1	**0.9**	0.1	0.9797	2.3821	1.2059
0.1	0.1	5.0	6.5	0.5	5.0	0.1	0.1	**3.0**	0.9653	4.7852	1.2059

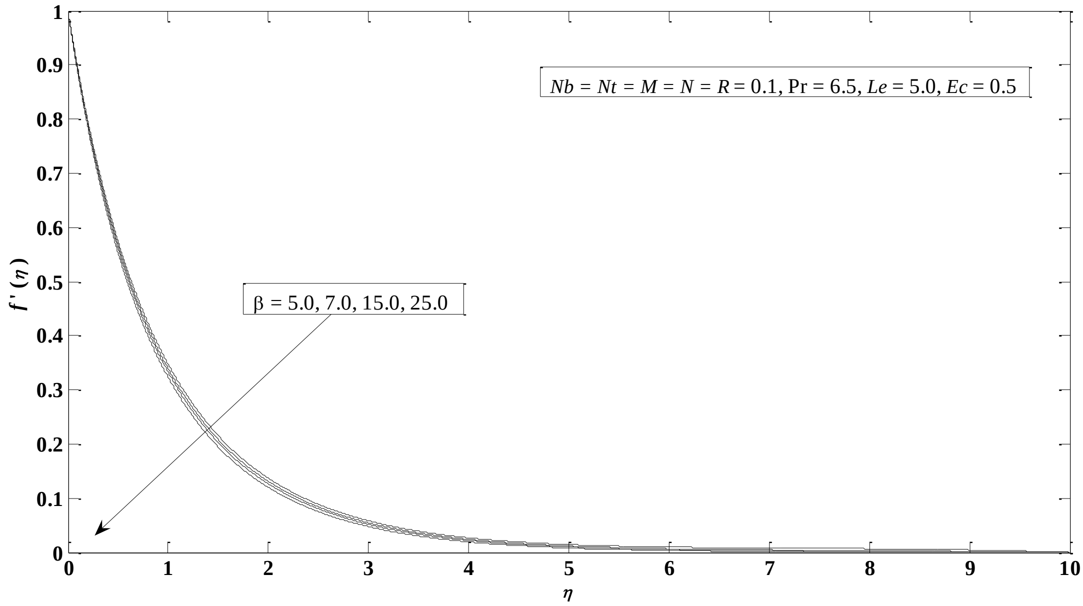

Figure 2: Velocity profile against η for different values of β.

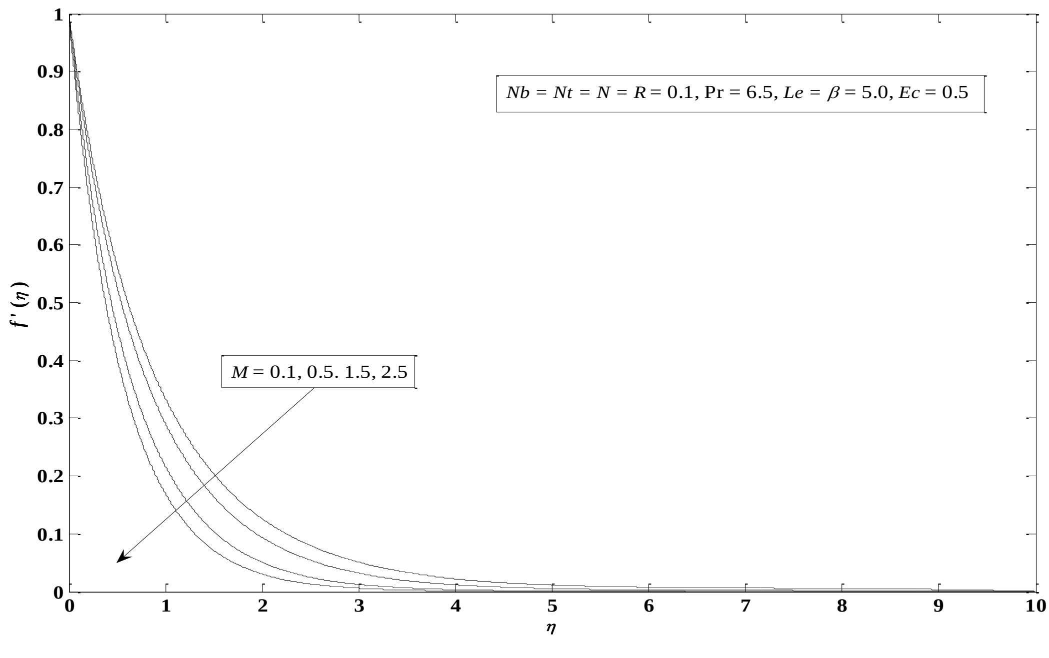

Figure 3: Velocity profile against η for different values of M.

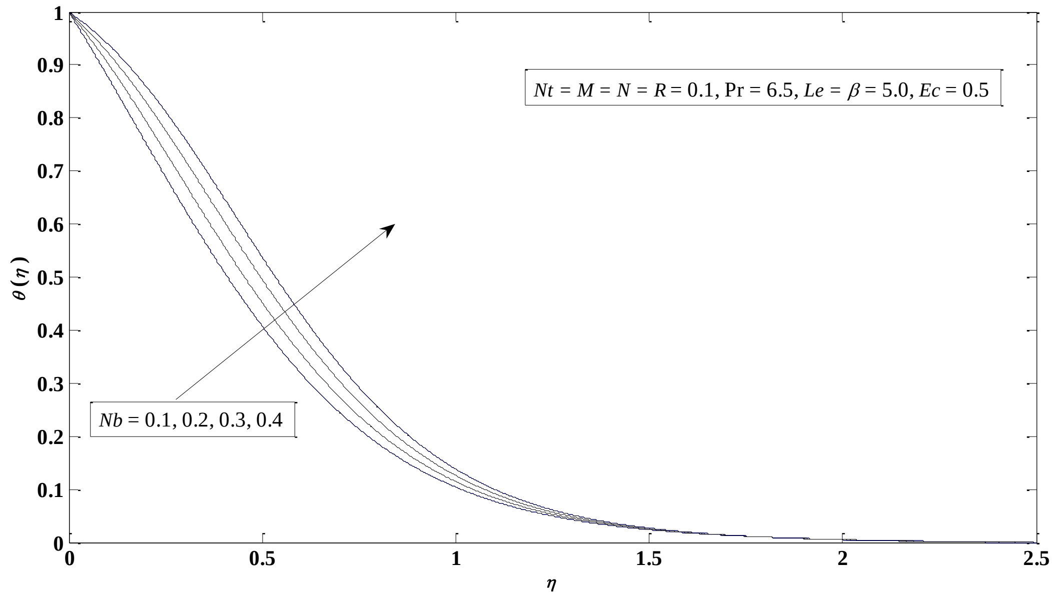

Figure 4: Temperature profile against η for different values of Nb.

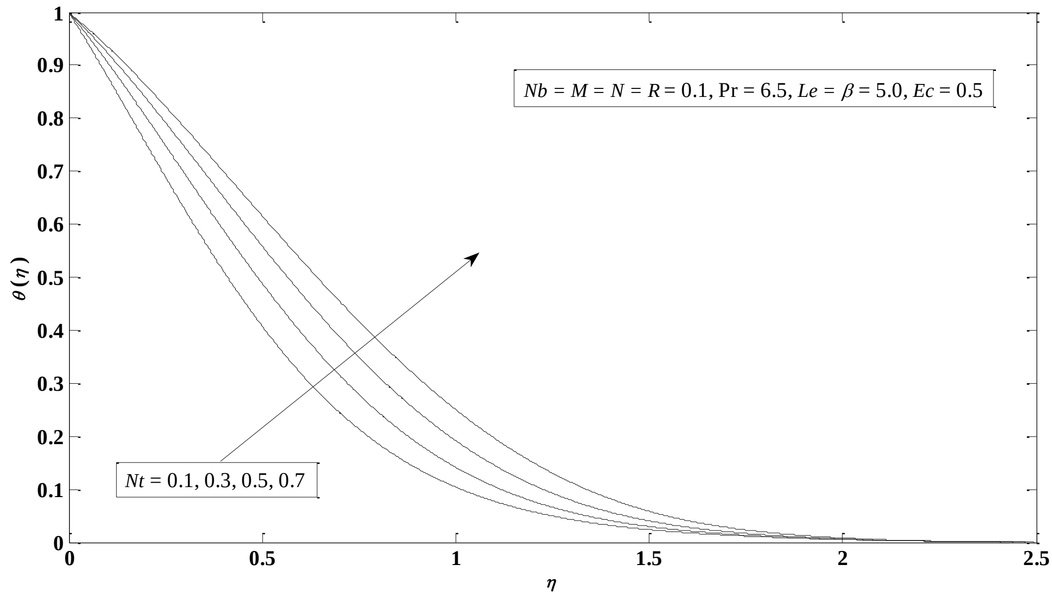

Figure 5: Temperature profile against η for different values of Nt.

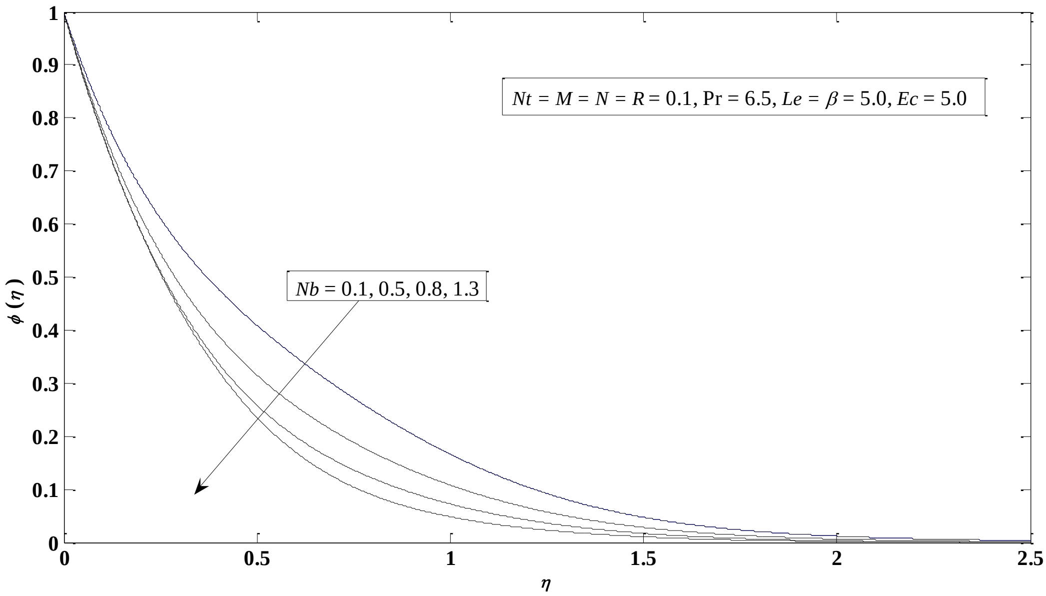

Figure 6: Concentration profile against η for different values of Nb.

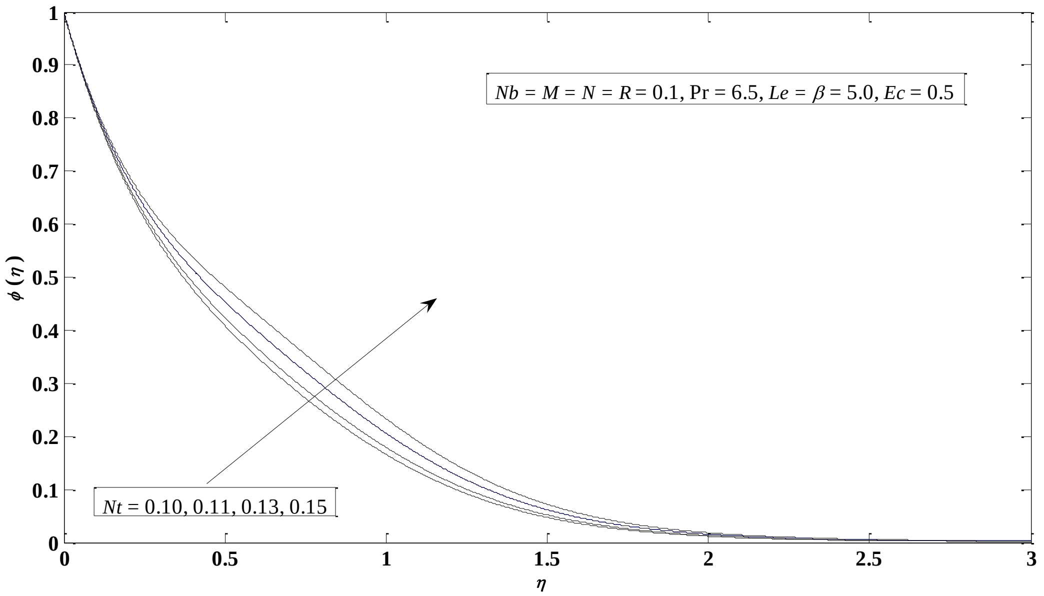

Figure 7: Concentration profile against η for different values of Nt.

Figure 2 depicts velocity profile for the different values of β by taking fixed values of *Nb, Nt, Le, M, N, R*, Pr and *Ec*. This behaviour is implicated because of the decreasing yield stress suppressed the velocity field. Figur 3 shows the effects of M on velocity profile $f'(\eta)$ for the fixed values of *Nb, Nt, N, R*,, Pr, *Le*, β and *Ec*. This figure shows that velocity profile $f'(\eta)$ decreases for increasing values of M. As M increases, the Lorentz force which opposes the flow, also increases and leads to enhance the deceleration of flow.

It is found from Figs. 4 and 5 that temperature profile increase for increasing values of *Nb* and *Nt* respectively. In nanofluid motions, particles gain the kinetic energy results for an increase in the collisions of particles. Therefore, $\theta(\eta)$ increases for increasing values of *Nb* and *Nt*.

Figures 6 shows decrease in concentration profile by increasing Brownian motion parameter Nb whereas increasing values of thermophoresis parameter Nt increases the concentration profile as shown in Fig. 7.

4. Conclusion

Present study numerically investigated the radiation and chemical reaction effects on Casson type MHD nanofluid flow over an exponentially stretching sheet. Non-Newtonian fluids with the involvement of Nanofluid have a great importance due to their superior properties and are beneficial in many fields. Flow phenomenon is characterized by different physical parameters and an analysis is made through graphical and tabulated data. These results can be extended for different flow geometries under different conditions.

It is observed that the reduced Nusselt number $-\theta'(0)$ decreases for increase in *Nb*, *Ec*, M, *R* whereas increases for increase in *Nt*, β, Pr, *Le* and *N*. Where the reduced Sherwood number $-\phi'(0)$ decreases for increase in *Nt*, β, *M*, *N* whereas increases for increase in *Nb*, Pr, *Ec*, *Le* and *R*. Further the skin-friction coefficient $C_{fx}(0)$ decreases for increase in Pr, *M*, *N* and increases for increase in β and *Le*.

5. References

[1] Buongiorno J., Convective transport in nanofluids. *J. Heat Transf,* **128**, (2006), pp. 240-250.

[2] Khan, W. A. and Pop, I,Boundary-layer flow of a nanofluid past a stretching sheet. *International Journal of Heat and Mass Transfer,* **53**, (2010), pp. 2477-2483.

[3] Xie W. Y., A Review on Nanofluids: Preparation, Stability Mechanisms, and Applications. *Journal of Nanomaterials,* **2012**, (2012).17.

[4] Motsumi, T. G. and Makinde, O. D., Effects of thermal radiation and viscous dissipation on boundary layer flow of nanofluids over a permeable moving flat plate. *Phys. Sci,* **86**, (2012), 8.

[5] Ravi S., *et al*., Effects of Some Parameters on Thermal Conductivity of Nanofluids and Mechanisms of Heat Transfer Improvemen. *IJERA,* **3**, (2013), pp. 2136-2140.

[6] Sakiadis, B. C., Boundary layer behavior on continuous solid surfaces: boundary layer equations for two-dimensional and axisymmetric flow. *AIChE Journal,* **7(1)** (1961), pp. 26-28.

[7] Erickson, L. E., *et al.,* Heat and mass transfer on a moving continuous flat plate with suction or injection, *Industrial and Engineering Chemistry Fundamentals,* **5(1)** (1966), pp. 19-25.

[8] Gupta, P. S. and Gupta, A. S., Heat and mass transfer on a stretching sheet with suction or blowing. *The Canadian journal of chemical Engineering,* **55(6),** (1977), pp. 744 - 746.

[9] Rajagopal, K. R., *et al.,* Flow of a viscoelastic fluid over a stretching sheet, *Rheol Acta,* **23**, (1984), pp. 213-215.

[10] Dutta, B. K., *et al.,* Temperature field in flow over a stretching sheet with uniform heat flux. *International Communication in Heat and Mass transfer,* **12,**(1985), pp. 89-94.

[11] Magyari, E. and Keller, B., Heat and mass transfer in the boundary layers on an exponentially stretching continuous surface. *Journal of Physics D: Applied Physics,* **32**, (1999), pp. 577-585.

[12] Bidin, B. and Nazar, R., Numerical solution of the boundary layer flow over an exponentially stretching sheet with thermal radiation. *European Journal of Scientific Research,* **33(4)**, (2009), pp. 710-717.

[13] Ishak A., MHD boundary layer flow due to an exponentially stretching sheet with radiation effect. *Sains Malaysiana* **40(4),** (2011), pp. 391-395.

[14] Animasaun I., Effect of thermophoresis, variable viscosity and thermal conductivity on free convective heat and mass transfer of non-darcian MHD dissipative Casson fluid flow with suction and nth order of chemical reaction . *Journalof Nigerian Mathematical society* **34,** (2015), pp.11-31.

[15] Animasaun I., Casson fluid flow with variable thermo-physical-property along exponentially stretching with suct ion and exponentially decaying internal heat generation using homotopy analysis method. *Journalof Nigerian Mathematical society* **35,** (2016), pp.11-31.